
Investigation of Chemical/Mechanical Polishing of Niobium

George Calota,^{*} Natalia Maximova⁺, Katherine S. Ziemer⁺, and Sinan Müftü^{*†}

^{*}Department of Mechanical Engineering

⁺Department of Chemical Engineering

Northeastern University

Boston, MA 02115

Submitted to *STLE Tribology Transactions*

on July 27, 2008, and in revised form on November 3, 2008

Abstract

A chemical/mechanical method for polishing flat niobium sheets to a mirror finish was developed. Various polishing slurries with different open circuit potentials and pH values were considered. All slurries fell within the niobate region of the Pourbaix diagrams, indicating that slurries are in a thermodynamically stable region. Oxidation characteristics of the niobium in the various slurries were determined by XPS, and confirmed previously published work that niobium forms various layers of stable niobium oxides roughly 4.5 – 4.7 nm in thickness on the surface. A multi-step polishing method which relies on mechanical abrasion of the surface proved to be effective, and particles of different hardnesses and size were explored. Niobium wafers with initial peak-to-valley (PV) surface roughness of 3 to 7 μm were polished. The multi-step process utilized a slurry containing 1 μm diameter alumina particles to polish this initial roughness down to a sub-micrometer level. The final polish was provided by a slurry containing smaller particles. The oxide slurry with 70-100 nm silica particles gave the best mirror finished surface, with PV = 235 nm, Ra = 32 nm and RMS = 39 nm. While polishing caused some disorder in the niobium metal, using the oxide-slurry gave results closer to those obtained by buffered chemical polish (BCP) which exhibit the highest degree of atomic order based on XPS studies. A polishing process starting with mechanical abrasion, followed by a two step mechanical polish, is successful for obtaining smooth niobium surfaces on flat wafers.

Keywords: Polishing, surface roughness, XPS

Descriptors: Niobium, chemical mechanical polishing, buffered chemical polishing, superconducting radio frequency cavities.

†Corresponding author: s.muftu@neu.edu, 617-373-4743/2921

INTRODUCTION

Linear particle accelerators are used in high energy particle physics experiments in order to energize subatomic charged particles. A key component of this type of particle accelerators is an electromagnetic cavity, resonating at microwave frequency, which accelerates the charged particles to very high velocities. The energy exchange between the radiofrequency (RF) cavity and the particle depends on the quality factor Q of the cavity, and on the accelerating field E_{acc} (Padamsee et al. (1)). Power dissipation from the walls of the cavities made of ordinary conductors, such as copper, affects the RF cavity performance. Considering that the surface resistance of a superconductor is five to six orders of magnitude lower than copper, cavities made of superconductor materials, or coated with superconductor materials are preferred in practice (Kneisel (2)). Niobium is favored above the other superconducting pure metals for the manufacturing of superconducting radio-frequency (SRF) cavities because: it has the highest critical transition temperature, $T_c = 9.2$ K; it has a sufficiently high critical magnetic field, $H_c > 2$ kOe; and its metallurgical properties are adequate for deep drawing the metal (Tian et al. (3)). Currently, a single cell SRF cavity is manufactured in two halves by deep drawing of high purity polycrystalline Niobium sheets that are few millimeters thick. Electronbeam (EB) welding is then used to form the full cavity from the two halves (Lilje et al. (4)).

The performance of a niobium-SRF cavity can suffer due to defects in the material, such as various forms of niobium-oxide layers near the surface, or the presence of other contaminants such as C or N, which cause high residual resistance and result in low Q values (Kneisel (2,5)). The surface of niobium is known to have several layers of niobium oxide (Grundner and Halbritter (6)). In particular, the metallic oxide NbO can adversely affect the superconductivity of the surface layer (Grundner and Halbritter (6)). Other metallic and organic contamination can diffuse into the material during handling and become segregated in the grain boundaries (Antoine et al. (7)). Another cause of niobium-SRF cavities' performance drop is reported to be enhanced field emission from surface defects such as scratches due to manufacturing and handling operations, and external contaminant particles deposited on the inner wall of the cavity (Kneisel (2,5); Wang et al. (8)). Indirect evidence of efficiency drop due to surface roughness is surmised by the lower Q drop in cavities with smoother surfaces (Wu et al. (8)). In order to avoid this negative impact on performance, up to 100 μm of the damaged surface layer is removed by a series of surface treatment methods (Kneisel (5)). These include: degreasing of the cavities to remove organic residues; Buffered chemical polishing (BCP), electropolishing (EP), and barrel rolling or polishing by tumbling a cavity full of abrasive particles in order to remove the damage layer and to polish the surface; high pressure rinsing in order to remove contaminant particles; high temperature ultra-high vacuum heat treatment in order to displace or remove hydrogen, oxygen and carbon from the niobium lattice (Daccà et al. (9)); and, *in-situ* baking at ~ 393 deg. K in order to condition the surface oxides (Ma et al. (10)).

Surface defects and contamination from forming and welding are typically removed with buffered chemical polish (BCP) and electrochemical polishing (EP). BCP process involves an acid mixture of phosphoric (H_3PO_4), hydrofluoric (HF) and nitric (HNO_3) acids with ratio of either 1:1:1 or 2:1:1 in order to etch away 100 μm or more of the damaged layer (Wu et al. (8)). BCP etches the grains of different orientation and the grain boundaries at different rates and results in an uneven surface, but a surface free of any mechanical damage or residual stress. The EP process involves material removal in an acid mixture under the flow of an electric current. A mixture of hydrofluoric (HF) and sulfuric (H_2SO_4) acids is used as the electrolyte. The cathode material is copper or aluminum. As the electric field is highest on the peaks of a rough surface,

the peaks dissolve faster than the valleys, and therefore depending on the initial peak-to-valley value, EP can be a slow process. However, a very glossy surface can be obtained with EP (Lilje et al (4)). Recently, Wu et al. (8) demonstrated that by using buffered electrical polishing the root mean square (RMS) roughness of the surface can be reduced to 35 nm. This is a sharp improvement in contrast to RMS of 251 nm and 1.3 μm obtained with EP and BCP, respectively. Perhaps one of the biggest drawbacks of BCP and EP is related to the use of harsh chemicals which impose strict handling, manufacturing, and disposal requirements.

Chemical mechanical polishing (CMP) has been effectively used in manufacturing of semiconductor devices for over 20 years to selectively remove material between various metal and dielectric deposition steps. The standard CMP process is performed by pressing and rotating a flat wafer against a rotating polishing pad and applying slurry containing abrasive particles and aqueous mixture of oxidizers, inhibitors, buffers, and stabilizers. The slurry chemistry is considerably less aggressive as compared to those contained in the solution used in BCP and EP.

In this paper, the results of a recent study on using chemical mechanical polishing in order to polish flat niobium sheets is reported. To the best of our knowledge this is the first report on CMP of niobium. Although this work has been carried out on flat wafers and whereas the SRF cavities have curved shapes, the results presented in this work for obtaining mirror-finish niobium surfaces lays down the necessary groundwork for understanding the critical aspects of the chemical mechanical polishing of niobium. The inherent advantage of the lack of harsh chemicals as part of the CMP process combined with the mirror-like finish and 39 nm RMS roughness of the niobium surface obtained in this feasibility study, suggests much promise for this technique.

MATERIALS AND METHODS

Flat niobium (Nb) wafers of 101.6 mm diameter, cut from rolled niobium sheets of 0.5 mm thickness were used in this study. These polycrystalline niobium samples were provided by H.C. Starck, Inc. (Newton, MA). The surfaces of these wafers were subjected to different manufacturing pre-treatment methods. This resulted in three groups of initial surface finish that were tested. The first group of wafers involved the untreated, or *as-rolled*, surface texture. The second group underwent a BCP treatment after being cut from the rolled sheet. The third group of wafers was subjected to mechanical abrasion prior to cutting in order to emulate the process known as “barrel rolling,” which is a preliminary surface treatment step in cavity manufacturing (Kneisel (5)). The starting surface morphology, shown in Figure 1, is quite different for all three pre-treatments. The untreated wafers, shown in Figure 1a, have deep, unidirectional scratches due the rolling operation. Visible grain structure in the surface profile of the BCP treated surface is shown in Figure 1b. This is expected, as it is known that different niobium grains are etched at different rates during the BCP treatment due to different lattice orientations. The barrel rolling process produced the lowest initial Peak-to-Valley (PV) value for the surface (Figure 1c) and removed the deep scratches from the initial rolling process.

Polishing was performed on a CMP tool (G&P Technologies Poli-500, Seoul, Korea). The rotational speeds of the wafer-carrier and the polishing pad were 60 rpm, and the wafer carrier was used in the standard linear oscillation mode of the instrument. The experiments were carried out by using 1 to 4 minute time intervals. At the end of each polishing interval, the polishing pad was reconditioned for 1 minute with a diamond reconditioning tool and the wafer was taken out of the CMP-machine. Once removed, the wafer was rinsed with water, dried with

nitrogen gas, and its weight and surface profile were recorded. A Mettler Toledo scale (model AG204 Delta Range, 0.1 mg readability) was used to measure the mass of the wafer. The surface profiles were obtained by using a Zygo NewView 6000 (Hartford, CT) optical profiler. The common surface roughness descriptors of peak-to-valley (PV), root-mean-square (RMS), and average roughness (Ra) were used to monitor the change of surface roughness throughout the polishing process. Once the surface roughness stopped changing between polishing intervals, the experiments were terminated. At the end of the polishing experiments, small samples (1 cm²) were cut from three regions of the wafer (center, edge and halfway between). These samples were analyzed using X-ray photoelectron spectroscopy (XPS) with a PHI Mg/Al dual anode, non-monochromatic X-ray source (model 04-173-0-007) and a PHI hemispherical analyzer (model 10-360-4-015). XPS analysis provided chemical composition of the surface to about 7 nm below the surface, based on the escape depth of Nb. All escape depths used for thickness calculations were modeled using the NIST database (15). XPS was used to identify the various oxide states of niobium through shifts in binding energy of the Nb 3d 5/2 and 3d 3/2 photoelectron peaks. Nb3d spectra were first fitted with metal and pentoxide peaks, with the pentoxide Nb₂O₅ shifted 5.1 eV to higher binding energy than the metal, per both literature ((Daccà et al (9); Ma and Rosenberg (14); Tian et al (3)) and current results. Nb 3d 3/2 and Nb 3d 5/2 doublets for both the metal and oxide were set 2.70 eV apart and ratio of the areas under the Nb 3d 3/2 peak to Nb 3d 5/2 was set to 0.66:1. Peak position for intermediate oxides (Nb_xO (1≤x≤2), and NbO₂) was corrected to give chemical shift to the higher energy from the metal peak of 1 eV for NbO_x (1≤x≤2) and 3.6 eV for NbO₂. An assigned Nb_xO peak instead of separate NbO and Nb₂O was used because of some discrepancies in peak identification in the literature (Daccà et al (9); Ma and Rosenberg (14); Tian et al (3)). Changes in the atomic order/disorder of the ~7 nm deep surface layer, was monitored through the changes in the full-width-half-max (FWHM) of the Nb 3d metal and oxide peaks, with a FWHM value of 1.1 eV as the limit of the instrument and representing the highest detectable level of atomic order. Surface morphology images were also captured through a JEOL JSM-6360 scanning electron microscope (SEM).

The different polishing slurries which were used in the experiments are summarized in Table 1. The slurries which primarily contain alumina particles are referred to as the *alumina slurry* and distinguished from one another by using the size of the alumina particles. One of the alumina slurries contained 50 nm polycrystalline alumina, and the other two slurries contained 0.5 μm and 1 μm calcinated alumina (Table 1). In addition to the alumina slurry, two slurries designed to polish SiO₂ were also used. These slurries, which contained colloidal silica particles, are referred to as the *oxide-slurry* in this work. The size of the colloidal silica particles are reported to be on the order of 50-100 nm (Table 1).

Some as-rolled niobium wafers were treated with BCP as part of understanding the surface oxidation and etching chemistry of the Nb, and as a pre-treatment to CMP processing. A standard BCP solution mixture, which consisted of hydrofluoric acid, nitric acid, and phosphoric acid (1:1:2), was used (Tian et al., (3); Liljie et al. (4)). BCP etching took place under a hood to remove evolving gases. For small samples used in static chemistry experiments, the Teflon beaker with the BCP solution was placed in a sonicator to ensure good mixing and even surface exposure. Full wafers processed as a pre-treatment to CMP, were agitated manually.

In this work, the interplay between the chemical changes caused on the surface by the slurry, and the abrasion of the surface due to particles was investigated. The effects of a) the slurry chemistry, b) the abrasive particle type and size, and c) the initial condition of the

Niobium surface on final polished surface roughness, chemistry, and morphology were considered. The experiments were carried out in two parts: a *preliminary study* and a *controlled study*. The *preliminary study* investigated the formation of Niobium oxide on the surface. This step was critical because it is generally believed that a metal oxide is softer, and hence easier to remove than the pure metal (Oliver (12)). The effects of several commercially available slurries, as well as buffered chemical polish (BCP), on surface chemistry were investigated. The slurries used in this work and their key properties are listed in Tables 1 and 2. This preliminary work also included various polishing tests involving pH adjustments and combinations of slurries and pre-treatments in multi-step processes. As described below, the results of the preliminary study suggested that effective polishing was dominated by mechanical abrasion of the surface, and a two-step process of an alumina slurry followed by an oxide slurry produced the most promising results. In the second part of this work a *controlled study* was conducted to determine the effects of some of the CMP parameters and pre-treatments on the outcome of polishing with the two-step process.

RELATIVE IMPACT OF CHEMICAL AND MECHANICAL PARAMETERS

Effects of Chemistry

Niobium, like tantalum, is a very corrosion-resistant metal. Tests of niobium in various acids of different concentrations and temperatures show very low corrosion rates (Sisco and Epremian (13)). However, niobium readily oxidizes forming NbO, NbO₂, and Nb₂O₅ oxides on the surface with Nb₂O₅ being the outermost layer (Grundner and Halbritter (6); Ma et al. (10)). Existence of the intermediate oxides is attributed to strain release caused by the large difference in densities of the metal and the pentoxide (Ma and Rosenberg (14)). The density of niobium and its oxides vary between 8.66 g/cm³ for the metal, and 4.3 g/cm³ for Nb₂O₅ (Fairbrother (16)). Metal CMP, unlike dielectric CMP, requires an oxidizing environment to form a metal-oxide which is softer than the metal in order to remove material with abrasive particles (Oliver, (12)). Based on the density values, one would expect niobium oxides to be softer than the bulk metal; therefore oxidation of the surface is desired.

Niobium oxide characteristics

The effects of an *oxidizer*, hydrogen peroxide, and an *etchant*, hydrofluoric acid, were determined through a series of experiments. 1 cm² samples cut from a rolled niobium wafer were submerged in different chemical environments for various time periods, and changes in surface chemistry were monitored by XPS. All the samples used were degreased. XPS analysis showed that the oxidized surfaces of the as-rolled wafers have a high degree of atomic scale disorder, as determined by a Nb_{NbxOy} 3d FWHM of 1.90 +/- 0.05 eV, and a Nb_{Nb2O5} 3d FWHM of 1.55 +/- 0.05 eV. The metal beneath the oxide is more ordered, with a FWHM of 1.30 +/- 0.05 eV. Hydrogen peroxide is a common oxidizing agent in copper CMP. For Nb, however, the concentration of hydrogen peroxide has no effect on the niobium oxide thickness. Nb₂O₅ thickness was calculated to be ~4.5 +/- 0.7 nm for 1%, 4.6% and 9.4% hydrogen peroxide concentrations, all exposed to the Nb surface for 10 minutes. This agrees with thicknesses observed previously (Grundner and Halbritter (6); Daccà et al (9); Ma and Rosenberg (14); Tian et al (3)). Hydrofluoric acid etching resulted in a decrease of niobium pentoxide thickness to ~4.1 +/- 0.6 nm. and a decrease in the metal FWHM from 1.30 +/- 0.05 eV to 1.20 +/- 0.05 eV. The oxide increased in thickness back to 4.6 +/- 0.7 nm during subsequent treatment with

hydrogen peroxide, and the FWHM of the metal peak returned to 1.30 +/- 0.05 eV. The similarity in thickness of the oxide layer formed in air (as received surface), after exposure to hydrogen peroxide, and after exposure to hydrogen peroxide after etching suggest a self-limiting oxide. While the decrease in Nb metal FWHM after etching suggests a removal of disordered metal layers, the increase in FWHM after exposure to hydrogen peroxide suggests possible non-uniform oxide layer formation (Darlinski and Hallbritter (17)) or serration (Hallbritter (18)).

The seemingly complete oxidation of the surface and near surface layers within 10 minutes suggest a very rapid surface oxidation. Four samples were first etched with hydrofluoric acid as described above in order to minimize the native oxide thickness on the surface. The samples were then treated with hydrogen peroxide for increasing time intervals of 10s, 30 s, 1 min and 30 min. The niobium oxide thickness of the samples were determined based on XPS measurements, and were found to be 4.5 +/- 0.7 nm for the 10 s exposure, and 4.6 +/- 0.7 nm for all of the other cases. This oxide is primarily Nb₂O₅. Thus, in hydrogen peroxide environment, niobium oxidizes readily and reaches an apparent self-limiting (within any time frame relevant to CMP) oxide 4.6 +/- 0.7 nm thick. The implication for CMP processing, is that material removal rate will most likely be controlled by mechanical abrasion and not chemical oxide formation.

Effect of buffered chemical polish

The material removal and change of surface roughness in buffered chemical polish (BCP) of 1cm² niobium pieces cut from as-rolled wafers was investigated in order to provide a comparison with the CMP process. No precaution to control the temperature of the mixture, which started at room temperature, was taken. The surface was characterized using the optical profiler and XPS. Figure 2 shows the amount of material removed and the surface roughness with respect to BCP exposure time. The PV surface roughness of niobium increased from 4.2 μm to 9.4 μm, with increased exposure to BCP up to 18 minutes, but with approximately half of that increase occurring in the first three minutes of exposure. However, the XPS analysis, presented in Figure 3, showed the full-width half-maximum (FWHM) of the BCP treated surface was reduced to 1.15 +/- 0.05 eV as compared to 1.60 +/- 0.05 eV of the untreated, as-rolled surface. This indicates that the BCP treatment removes the disordered metal layers from the surface of the as-received wafer, but at the cost of increased surface roughness. As this increased surface roughness is attributed to differential etching of the faces of different grains and the grain boundaries, a CMP process that removed the disordered surface layers while maintaining a smooth surface would be advantageous.

Note that the material removal rate of this BCP operation, in the 3-18 minutes range shown in Figure 2, can be computed as 1.5 μm/minute, by using $\Delta h/\Delta t = \Delta m/(\rho_{Nb} A \Delta t)$ with $\rho_{Nb} = 8.66 \text{ gr/cm}^3$, and $A = 1 \text{ cm}^2$, $\Delta t = 15 \text{ minutes}$. This is higher than the 1 μm/minute rate reported by Lilje et al. (4) for mixtures at 10 deg. C. This difference in removal rates is attributed to the difference in the operating temperature.

Pourbaix diagrams

Corrosion of metals in aqueous solutions was extensively studied by Pourbaix who developed thermodynamic equilibrium diagrams (Pourbaix (19)). The Pourbaix diagrams provide information of immunity, passivity, and corrosion of materials. By changing pH and solution potential, one changes thermodynamic equilibrium. If conditions are changed sufficiently, different surface species may be favored and start forming. This is of interest in the

CMP process because although the overall oxidation rate is rapid and not the limiting step, the different densities of the different Nb oxide species suggest possible differences in physical removal rates.

The initial niobium Pourbaix diagram lacks transition lines between niobic acid and niobium pentoxide, and between niobate and niobium pentoxide (Pourbaix (19)). Recently, Asselin et al. (20) published the Pourbaix diagram of niobium shown in Figure 4, in aqueous solutions of sulfuric and hydrochloric acids. This diagram shows that the region for niobium metal lies below all forms of Nb_xO_y in water, which indicates that niobium will oxidize in any aqueous solution. This further supports the conclusion that oxidation rate will not be a factor in CMP processing time, but rather physical abrasion and/or dissolution will determine material removal rates.

The vertical line at pH of ~ 6.5 of Figure 4 indicates that at pH values lower than this, Nb_2O_5 is thermodynamically favored, while at higher pH values niobate (NbO_3^-) will be favored. The open circuit potential (OCP) and the pH of the slurries used in this work are given in Table 1. Oxide and Cu slurries, with pH ~ 10 , operate in the niobate region of the Pourbaix diagram, while the alumina polish, with a pH of ~ 6.8 , operates close to the vertical equilibrium line between Nb_2O_5 and niobate. In order to separate the impact of pH from particle differences, the pH of the alumina polish was adjusted to 10 using sodium hydroxide. However, neither the oxide nor the aluminum slurries could be chemically adjusted into the niobate equilibrium region without coagulating particles of the slurry. Thus, although we could experiment with the same slurry (alumina slurry) at two pH values of ~ 6.9 and 10, all slurries tested were within the same equilibrium region of the Pourbaix diagram as shown in Figure 4. No conclusive differences in CMP results occurred from the adjustment of slurry pH.

Preliminary Polishing Experiments

Initial polishing experiments involved using either a copper-slurry or an oxide-slurry (Table 1). These experiments showed that the surface roughness is somewhat reduced, but the rate of reduction slows down with increasing polishing time. These results are reported by Calota (21) in detail, but omitted from this paper due to space considerations. This result is attributed, first, to the stable nature of the niobium-oxide as described above, and also to the nature of the abrasive particles in these slurries. Both of these slurries contain colloidal silica, a relatively soft abrasive (Table 1). The combined effects of using relatively soft particles, ineffective chemistry, and large initial surface roughness lead to poor material removal characteristics using the copper- and oxide-slurries.

A TWO-STEP POLISHING PROCESS

Once the stability of Nb_xO_y was determined, mechanical abrasion was emphasized to remove the bulk of the surface roughness. Slurries containing alumina particles with relatively large (0.5 and 1 μm) diameters were used to remove the bulk of the material from the surface (Table 1). The effectiveness of using slurries with smaller (50-100 nm) particles for the finishing operation was then tested by using the oxide and 50-nm-alumina slurries indicated in Table 1.

Three groups of niobium wafers whose initial surface were *as-rolled*, *BCP-treated* and *mechanically-abraded* as mentioned above were used. The conditions of these seven polishing tests are reported in Table 2.

Evolution of Surface Roughness

The variations of the surface roughness measures PV, Ra and RMS were monitored during the experiments. Representative surface profiles of the initial surface roughness are given in Figure 1, and the initial roughness values of the three types of starting surface are reported in Table 3. As seen in Table 3, the as-rolled and BCP-treated surfaces had very similar initial roughness values, whereas the mechanically-abraded wafers had lower roughness values. This is important because the total reduction of the PV roughness may be faster if starting from lower initial PV values.

Figure 5 shows “snap-shots” of the surface roughness during Test-1 measured at 0, 42, 60 and 72 minutes. This wafer initially had the untreated, rolled surface, with a PV roughness of 7.16 μm and RMS roughness of 1.05 μm as reported in Table 3. Note that the initial scratches attributed to the rolling operation, shown in Figure 5a, render the initial roughness anisotropic. Figure 6 shows the change of PV, RMS and Ra roughness of this surface during the test, along with the type of slurry, and the corresponding down pressure used during polishing. The initial PV roughness persists for about 6 minutes of polishing with the 0.5 μm alumina slurry, and then decreased slowly but steadily from 7.16 μm to 0.75 μm using both the 0.5 μm and 1 μm alumina slurry. The final polish with the oxide-slurry, further reduces the PV to 0.22 μm . Figure 5b shows that after 42 minutes of polishing the initial rolling-marks are still visible on the surface, whereas they disappear after 60 minutes. The final values of the PV, RMS and Ra roughness of this wafer were 0.218 μm , 34 nm and 28 nm, respectively, as shown in Figure 6 and Table 3.

The progression of surface roughness change for the wafers initially treated with BCP, in Tests-2,-3 and -4, are presented in Figure 7. The BCP treatment removes the rolling marks, and exposes the grain boundaries as shown $t = 0$ in Figure 1b. The starting PV roughness is on the order of 7 μm for these three wafers as reported in Table 3. Figures 7a, 7c, and 7e report that 0.5 and 1 μm diameter alumina slurries were used initially to remove the bulk of the roughness. Note that the 1 μm -alumina slurry was far more effective in this step as compared to the 0.5 μm -alumina slurry. This is attributed to agglomeration in the 0.5 μm -alumina slurry, which was noted after the tests were completed. The 1 μm -alumina slurry effectively reduces the PV roughness from ~ 7 μm to ~ 1 μm after 10 minutes of polishing. Effects of using the oxide slurry, the 50 nm alumina-slurry with the as received pH, and the 50 nm alumina slurry with the adjusted pH value of 10 in the finishing step are shown in Figures 7a, 7c, and 7e. Close inspection of these figures and the results summarized in Table 3 shows that the oxide slurry is more effective in obtaining a smoother surface at the final step.

The PV roughness of the wafers which were initially treated with mechanical abrasion before Tests-5, -6 and -7 were on the order of 3-4 μm , and these surfaces appeared relatively more isotropic, as shown in Figure 1c. The changes of surface roughness of these three wafers are presented in Figure 8. The first step consisted of 10 minutes of polishing with the 1 μm -alumina slurry which reduced the PV roughness to $\sim 1\mu\text{m}$. The push-down pressure in this step was 800 g/cm^2 as shown in Figures 8b, 8d and 8f. The results of polishing by using the oxide slurry, and the as received and pH-adjusted 50-nm alumina slurries show that the oxide slurry reaches the lowest RMS roughness in the shortest time. Note that the push down pressure had to be adjusted during these tests from 800 gr/cm^2 to 500 gr/cm^2 as the surface roughness change was not progressing smoothly.

Based on these results we see that the three wafers finished with the oxide-slurry, (tests-1,-2, and -5) resulted in considerably smoother surfaces, as compared to the four wafers finished with the 0.05 μm Alumina-slurry, (tests-3, -4, -6, and -7). Table 3 shows that the polishing operation levels off at PV roughness of 0.41 μm and 0.24 μm , and RMS roughness of 87 nm and 39 nm for the 50 nm alumina-slurry and the oxide -slurry, respectively. Moreover, the limited number of tests performed here showed that neither the initial surface preparation, nor the pH of the slurries had as significant an effect as the type of the final slurry.

The slurries used in the experiments listed in Table 1 involved three types of particles: colloidal-silica in the oxide-slurry and polycrystalline alumina in the 50-nm-alumina slurry and calcinated alumina in the 1 μm -alumina slurry. The experiments showed that the 1 μm calcinated alumina particles are more effective in removing relatively large amounts of material as compared to the colloidal silica particles. The amount of material removed in test-2 - test-7 was monitored during the tests and reported in Figure 7 and 8. Based on these results, a material removal rate can be calculated for the different slurries. The material removal rate (MRR) in CMP is generally expressed by Preston's equation, which states that it depends linearly on the average polishing pressure P and relative sliding speed V , as follows:

$$\text{MRR} = k_p PV \quad (1)$$

where k_p is the (*Preston*) *wear coefficient* which represents the combined effects of slurry chemistry, and hardness of the polished surface. The MRR and P values are reported on Figures 7b,d,f and 8b,d,f. The wear coefficients based on these experiments are computed and reported in Table 5. Using the average push down pressure and the polishing speed values for each test, and the material removal data presented in Figure 7 and 8, k_p is found to be $4.8 \times 10^{-7} \text{ gr.}(\text{Pa.m})^{-1}$ for the 1 μm alumina particles, $2.2 \times 10^{-7} \text{ gr.}(\text{Pa.m})^{-1}$ for the 50 nm alumina particles, and $1.5 \times 10^{-7} \text{ gr.}(\text{Pa.m})^{-1}$ for the silica particles. While clearly more experiments are required to establish more reliable wear coefficient values, these findings confirm, in these first organized tests of niobium-CMP, that larger and harder alumina particles (Table 1) are suitable for removing the bulk of the initially surface roughness.

End Conditions

A qualitative comparison of unpolished and polished niobium wafers is given in Figure 9. The polished (two step process with oxide slurry in the final step) wafer shown on the right is nearly mirror smooth, evidenced by the good reflection. While all of the wafers polished with the oxide-slurry in the last polishing step had a similarly good finish, a white residue was observed on the surface of the wafers finished with the 50 nm alumina slurry, despite the fact that all the wafers dried by the same procedure after the last step.

SEM images of the surfaces showed a large concentration of particles on the wafers finished with the 50 nm alumina-slurry. Figure 10 shows two images representative of typical oxide-finish (a) and alumina finish (b). The XPS analysis of the surfaces, presented in Table 4, showed the presence of aluminum oxide for the test-3, -4, -6 and -7, whereas only small amounts of silica-particles were detected by XPS tests-1,-2 and -5, finished with oxide slurry.

The SEM pictures also show that the alumina-particles agglomerate on the surface, rather than appearing individually. The zeta-potential of the 50-nm-alumina slurry was measured as -18.6 mV at pH of 9.5, while that of the silica containing slurry was -110 mV at pH 10. The low zeta-potential combined with the lack of cleaning agents in the 50-nm-alumina slurry could be

responsible for agglomeration of the alumina particles. Agglomerated particles with increased surface area would have a higher chance to adhere on to the niobium surface. Deposition of abrasive particles on the polished surface is a known problem in CMP. The addition of surfactants in the slurry and post-CMP cleaning operations such as brush cleaning and ultrasonic cleaning aim to remove these particles from the surface.

Chemical Uniformity of the Polished Niobium

As described above, 1 cm² samples were cut from three different radial locations on the wafer: the center, the edge, and approximately half way in between. No significant difference was observed as a function of sample location, thus implying a uniform treatment by the CMP process over the entire wafer. Thus, Table 4 presents the average values of the XPS results obtained from the three locations. Table 4 compares experiments where the major CMP processing difference was the final slurry choice (oxide or 50 nm alumina slurry) and also contains the XPS results of a niobium sample treated with 6 minutes of BCP. The most notable differences between the final surface finish of the oxide versus alumina slurry, are the high aluminum contamination of the surface after the alumina slurry, the more ordered near-surface after the oxide slurry treatment, and the thinner and apparently different composition of the oxide layer after the oxide slurry treatment.

The full-width half-maximum (FWHM) of the Nb 3d peaks represent the level of atomic range order of the bonding states. Thus, the smaller FWHM values represent a more ordered bonding environment, and more homogeneous surface. From Table 4, the wafers finished with the oxide-slurry consistently have lower FWHM values than the wafers polished with alumina-slurry only. This indicates that either the oxide-slurry is more efficient at removing damaged layers from previous processing steps, or that the oxide-slurry polishing does not damage the surface to the extent that the alumina polish damages the surface. Note that the most ordered surface at the atomic level, is the BCP treated sample.

Comparison of the values reported in Table 4 suggests that the CMP does create some disorder in the atomic scale structure regardless of slurry. Nevertheless, the FWHM values across slurries shows that the mirror finish samples (tests-1, -2, -5) have the best ordered surfaces closer to the values obtained by the 6 minute BCP treatment.

The initial surface treatment did not have significant influence in the quality of the final surface finish. Nevertheless, it should be noted that it took a shorter time, to polish the surfaces which were mechanically abraded, and which had lower initial PV roughness. Our BCP treatment experiments consistently gave PV roughness values that are on the order of 7 μm. Polishing of wafers that were initially treated with BCP, required a longer processing time with the 1-μm-alumina slurry to remove the initial rough layer. It appears that a general process starting with mechanical abrasion (barrel rolling) followed by a polishing operation as described here will be successful for obtaining mirror-smooth niobium surfaces.

SUMMARY AND CONCLUSIONS

A method for polishing flat niobium sheets was developed. Experiments have been carried out to determine the oxidation characteristics of niobium and confirmed the previous work that niobium forms a stable oxide of mostly niobium pentoxide roughly 4.5 – 4.7 +/- 0.7 nm in thickness on the surface. Various polishing slurries have been considered, with respect to

their open circuit potentials, pH values, particle size, and particle type. Upon determining that niobium quickly forms stable, self-limiting oxide that is in a stable region of the Pourbaix diagram and cannot be shifted from this stable region without coagulating particles in the slurry, a multi-step polishing method which relies on mechanical abrasion of the surface utilizing particles of different hardness was explored. Initial PV surface roughness of the niobium wafers varies between 3 to 7 μm depending on the method of preparation. The multi-step process utilized a slurry containing 1 μm diameter alumina particles to polish this initial roughness down to a sub micrometer level. The final polish is provided by a slurry containing smaller particles. The oxide slurry with 70-100 nm silica particles gave the best mirror finished surface with PV = 235 nm, Ra = 32 nm and RMS = 39 nm. The 50 nm-alumina slurry polished the surface to slightly higher values and also left a residue of alumina particles on the surface. The XPS FWHM of the Nb peaks decreased from 1.6 +/- 0.05 eV to ~1.3 +/- 0.05 eV, showing the most ordered surface for the wafers finished with oxide-slurry. While polishing causes some disorder in the niobium metal, using the oxide-slurry gives results closer to those obtained by BCP which exhibit the highest degree of order with a FWHM of 1.15 +/- 0.05 eV. This work showed that a general process starting with mechanical abrasion (barrel rolling) followed by a two step process utilizing harder alumina followed by softer silica particles is successful for obtaining smooth, mirror-finish surfaces on flat niobium wafers.

It is interesting to note that RMS roughness of the Nb surface treated by buffered electropolishing (Wu et al. (8)), and by CMP are 35 and 39 nm, respectively. More controlled experiments are required to determine if this is a lower limit for the Nb surface. Finally, chemical mechanical polishing of concave Nb surfaces in RF-superconducting cavities remains to be demonstrated. Until then the RF-response of the CMP treated Nb-wafers will remain unknown.

ACKNOWLEDGEMENTS

This work was sponsored in part by H.C. Starck, LLC, (Newton, MA, USA) and in part by the National Science Foundation (Award # NSF-0425826). Part of this work was carried out in the facilities of the George J. Kostas Nanoscale Technology and Manufacturing Research Center at Northeastern University (NEU). The authors would like to acknowledge the discussions with Mr. Peter Jepson (H.C. Starck), Professor E. Podlaha-Murphy (Chemical Engineering Department, NEU) and Dr. Nam-Goo Cha (NSF-Center for High-rate Nanomanufacturing, NEU) during the course of this work, and thank Professor A. Sacco (Chemical Engineering Department, NEU) for the use of the scale and scanning electron microscope.

REFERENCES

1. Padamsee, H., Knobloch, J. and Hays, T. (1998), "RF Superconductivity for Accelerators," John Wiley and Sons, Inc, New York, USA.
2. Kneisel, P. (1999), "High Gradient Superconducting Niobium Cavities. A Review of The Present Status," Applied Superconductivity, IEEE Transactions on, **9**, 2, pp. 1023-1029.
3. Tian, H., Reece, C.E., Kelley, M.J., Wang, S., Plucinski, L., Smith, K.E. and Nowell M.M. (2006), "Surface Studies of Niobium Chemically Polished Under Conditions for Superconducting Radio Frequency (SRF) Cavity Production," Applied Surface Science, **253**, 3, pp. 1236-1242.
4. Lilje, L., Antoine, C., Benvenuti, C., Bloess, D., Charrier, J.-P., Chiaveri, E., Ferreira, L., Losito, R., Matheisen, A., Preis, H., Proch, D., Reschke, D., Safa, H., Schmäser, P., Trines, D., Visentin, B. and Wenninger H. (2004) "Improved Surface Treatment of the Superconducting TESLA Cavities," Nuclear Instruments & Methods in Physics Research, Section A: Accelerators, Spectrometers, Detectors, and Associated Equipment, **516**, 2-3, pp. 213-227.
5. Kneisel, P. (2006), "Cavity Preparation/Assembly Techniques and Impact on Q, Realistic Q-Factors In A Module, Review of Modules," Nuclear Instruments & Methods in Physics Research, Section A: Accelerators, Spectrometers, Detectors, and Associated Equipment, **557**, 1, pp. 250-258.
6. Grundner, M. and Halbritter, J. (1980) "XPS and AES Studies on Oxide Growth and Oxide Coatings on Niobium," Journal of Applied Physics, **51**, 1, pp. 397-405.
7. Antoine, C, Bonin, B., Safa, H., Berthier, B., Tessier, C., Tocellier, P., Chevarier, A., Chevarier, N. and Roux, B. (1997), "Evidence of Preferential Diffusion of Impurities Along Grain Boundaries In Very Pure Niobium Used For Radio-Frequency Cavities," Journal of Applied Physics, **81**, 4, pp. 1677-1682.
8. Wu, A.T., Mammosser, J., Phillips, L., Delayen, J., Reece, C., Wilkerson, A., Smith, D. and Ike, R. (2007), "Smooth Nb surfaces fabricated by buffered electropolishing," Applied Surface Science, **253**, 6, pp. 3041-3052.
9. Daccà, A., Gemme, G., Mattera, L. and Parodi, R. (1998), "XPS Analysis of the Surface Composition of Niobium for Superconducting RF Cavities," Applied Surface Science, **126**, 3-4, pp. 219-230.
10. Ma, Q., Ryan, P., Freeland, J.W. and Rosenberg, R.A., (2004), "Thermal Effect on the Oxides On Nb(100) Studied by Synchrotron-Radiation X-Ray Photoelectron Spectroscopy," Journal of Applied Physics, **96**, 12, pp. 7675-7680.
11. Wang, T., Reece, C.E. and Sundelin, R.M. (2003) "Enhanced Field Emission From Chemically Etched and Electropolished Broad-Area Niobium," Journal of Vacuum Science & Technology, B: Microelectronics and Nanometer Structures--Processing, Measurement, and Phenomena, **21**, 4, pp. 1230-1239.
12. Oliver, M.R. (2004), "Chemical-Mechanical Planarization of Semiconductor Materials," Springer Publishing Company, New York, U.S.A., p. 425.
13. Sisco, F.T. and Epremian E. (1963), "Columbium and Tantalum," Wiley, New York, USA.

-
14. Ma, Q. and Rosenberg, R.A. (2003), "Angle-Resolved X-Ray Photoelectron Spectroscopy Study of the Oxides on Nb Surfaces for Superconducting R.F. Cavity Applications," *Applied Surface Science*, **206**, 1-4, pp. 209-217.
 15. NIST: NIST Database 82, version 1.0, U.S. Department of Commerce (2001).
 16. Fairbrother, F., (1967) "The Chemistry of Niobium and Tantalum," Elsevier Publishing Company, New York, USA.
 17. Darlinski, A. and J. Halbritter, Angle-resolved XPS studies on oxides at niobium mononitride, niobium monocarbide, and niobium surfaces. *Surface and Interface Analysis*, 1987. 10(5): p. 223-37.
 18. Halbritter, J., On the oxidation and on the superconductivity of niobium. *Applied Physics A: Materials Science & Processing*, 1987. 43(1): p. 1-28.
 19. Pourbaix, M. (1966) "Atlas of Electrochemical Equilibria in Aqueous Solutions," Pergamon Press, New York, USA. pp. 246-250.
 20. Asselin, E., Ahmed, T.M. and A. Alfantazi (2007), "Corrosion of Niobium in Sulfuric and Hydrochloric Acid Solutions at 75 and 95 deg. C," *Corrosion Science*, **49**, 2, pp. 694-710.
 21. Calota, G. (2007), "Chemical Mechanical Planarization: A Three Dimensional Mathematical Model and Development of a Process for Polishing Niobium," Masters Thesis 2007, Northeastern University, Department of Mechanical and Industrial Engineering, Boston, MA, USA.
 22. PACE Technologies (2007), "Data Sheet," 1802 W. Grant Rd., No. 102, Tucson, AZ, 85745.

| Slurry | Supplier | Particle Type/Size | Particle Conc. | Hardness (Mohs) | OCP (V) | pH |
|------------------------------|------------------------------------|-----------------------------------|-----------------------|------------------------|----------------|-----------|
| Cu-slurry | Cabot EP-C6678 | Colloidal silica/ 90 -140 nm | N.A. ³ | 6-7 ¹ | -0.375 | 9.82 |
| Oxide-slurry | EKC, Microplanar CMP1150 | Colloidal silica/ 50-100 nm | N.A. ³ | 6-7 ¹ | - 0.5142 | 10.54 |
| Oxide-slurry | M&S Technologies Nalco 2398 | Colloidal silica/ 70-100 nm | 28% weight | 6-7 ¹ | | |
| Alumina slurry-50 nm | Pace Technologies NA-1005-128 | Polycrystalline alumina/ 50 nm | 20% weight | 9 ² | | |
| Alumina slurry-1 μm | Pace Technologies NANO-1010-128 | Calcinated alumina/ 1 μm | 20% weight | 9 ² | - 0.2379 | 6.73 |
| Alumina Slurry-0.5 μm | Pace Technologies NANO-1105-128 | Calcinated alumina/ 0.5 μm | 20% weight | 9 ² | 0.2141 | 6.02 |

Table 1: Properties of the slurries and suspensions used in the experiments. ¹(Oliver (12)), ²(Pace technologies (22)), ³not available.

| Test No. | Initial Surface | Initial polish | | | | | | Final polish | | |
|----------|-----------------|--------------------|----|-------|----------------------|----|-------|--------------|-------|-----------|
| | | Slurry-1 | pH | Conc. | Slurry-2 | pH | Conc. | Slurry-3 | pH | Conc. |
| 1 | As rolled | alumina -1 μ m | 7* | as is | alumina -0.5 μ m | 7* | as is | oxide | 10* | as is |
| 2 | BCP | alumina -1 μ m | 7* | 11% | alumina -0.5 μ m | 7* | 11% | oxide | 10.5* | as is |
| 3 | BCP | alumina -1 μ m | 7* | 11% | - | - | - | alumina-50nm | 7* | 50%dilute |
| 4 | BCP | alumina -1 μ m | 10 | 11% | alumina -0.5 μ m | 10 | 11% | alumina-50nm | 10 | 50%dilute |
| 5 | Mech. Abr. | alumina -1 μ m | 7* | 11% | - | - | - | oxide | 10.5* | 11% |
| 6 | Mech. Abr. | alumina -1 μ m | 7* | 11% | - | - | - | alumina-50nm | 7* | 50%dilute |
| 7 | Mech. Abr. | alumina -1 μ m | 10 | 11% | - | - | - | alumina-50nm | 10 | 50%dilute |

*The original PH values are not changed

Table 2: The pH values of the slurries used in the experiments.

| Test | Final Slurry | Initial Surface | Before polishing | | | After polishing | | | |
|------|---------------|---------------------|----------------------|-----------------------|----------------------|----------------------|-----------------------|----------------------|-------|
| | | | PV (μm) | RMS (μm) | Ra (μm) | PV (μm) | RMS (μm) | Ra (μm) | |
| 1 | Oxide | As-rolled | 7.161 | 1.053 | 0.817 | 0.218 | 0.034 | 0.028 | |
| 2 | Oxide | BCP | 7.774 | 1.024 | 0.848 | 0.247 | 0.051 | 0.043 | |
| 5 | Oxide | Mechanical abrasion | 3.354 | 0.386 | 0.306 | 0.240 | 0.033 | 0.026 | |
| | | | | | | Average | 0.235 | 0.039 | 0.032 |
| | | | | | | St. dev. | 0.015 | 0.010 | 0.009 |
| 3 | alumina-50 nm | BCP | 7.283 | 0.925 | 0.775 | 0.434 | 0.092 | 0.075 | |
| 4 | alumina-50 nm | BCP | 6.811 | 1.144 | 0.952 | 0.404 | 0.079 | 0.064 | |
| 6 | alumina-50 nm | Mechanical abrasion | 4.322 | 0.461 | 0.364 | 0.468 | 0.11 | 0.093 | |
| 7 | alumina-50 nm | Mechanical abrasion | 3.826 | 0.398 | 0.316 | 0.354 | 0.073 | 0.061 | |
| | | | | | | Average | 0.409 | 0.087 | 0.073 |
| | | | | | | St. dev. | 0.048 | 0.016 | 0.014 |

Table 3: The initial and final values of the surface roughness measures PV, RMS and Ra organized according to the slurry used in the final finishing step.

| Test | Final Slurry | Relative Elemental composition | | | | | FWHM (eV) | | | |
|------|---------------|--------------------------------|----|----|----|----|-----------|-----------|-------------------------------------|-----------|
| | | O | C | Nb | Al | Si | Metal | Oxides | Nb _x O _y (nm) | Nb/O |
| 1 | Oxide | 51 | 25 | 21 | | 3 | 1.30-1.35 | 1.50-1.55 | 4.7 | 0.37-0.46 |
| 2 | Oxide | 53 | 24 | 23 | | | 1.20 | 1.50-1.55 | 4.6 | 0.37-0.49 |
| 5 | Oxide | 51 | 28 | 21 | | | 1.40 | 1.50 | 4.8 | 0.39 |
| 3 | alumina -50nm | 53 | 22 | 13 | 12 | | 1.60 | 1.60 | 4.9 | 0.23-0.25 |
| 4 | alumina -50nm | 55 | 19 | 13 | 13 | | 1.60 | 1.60 | 4.9 | 0.22-0.25 |
| 6 | alumina -50nm | 55 | 20 | 14 | 12 | | 1.60 | 1.60 | 4.9 | 0.24-0.29 |
| 7 | alumina -50nm | 53 | 21 | 13 | 13 | | 1.50 | 1.50 | 4.9 | 0.22-0.26 |
| | 6 min. BCP | 47 | 28 | 25 | | | 1.15 | 1.60 | 4.1 | 0.52 |

Table 4: Relative elemental composition, full width half-maximum (FWHM), oxide thickness and niobium to oxygen ratios obtained by XPS analysis of polished samples. The polishing results are compared to a niobium sample treated with BCP for 6 minutes. The elemental composition and thickness of Nb_xO_y are average values for 1cm² samples cut from the center middle and outer edge of the polished wafers. Minimum and maximum values for FWHM and Nb/O ratio are shown where variation was observed.

| Slurry type | Alumina- 1 μm | Alumina- 0.5 μm | Alumina-50 nm | | | Oxide | | |
|-----------------|-----------------------------|-------------------------------|---------------|----------|----------|----------|----------|----------|
| Pressure (kPa) | 80.8 | 80.8 | 80.8 | 50.5 | 50.5 | 80.8 | 50.5 | 30.3 |
| Speed (rpm) | 60 | 60 | 60 | 60 | 100 | 60 | 60 | 60 |
| Test | | | | | | | | |
| 2 | 4.42E-07 | 5.04E-08 | | | | | 1.74E-07 | 1.86E-07 |
| 3 | 3.72E-07 | | 2.91E-07 | 4.47E-10 | | | | |
| 4 | 4.34E-07 | 6.20E-08 | 2.33E-07 | | 2.27E-07 | | | |
| 5 | 5.00E-07 | | | | | 9.31E-08 | | |
| 6 | 5.12E-07 | | 2.68E-07 | | | | | |
| 7 | 6.01E-07 | | 3.14E-07 | | | | | |
| Average k_p | 4.77E-07 | 5.62E-08 | 2.22E-07 | | | 1.51E-07 | | |
| St. dev., k_p | 7.89E-08 | 8.23E-09 | 1.14E-07 | | | 5.05E-08 | | |

Table 5: The wear coefficients k_p based on the results reported on Figures 7 and 8.

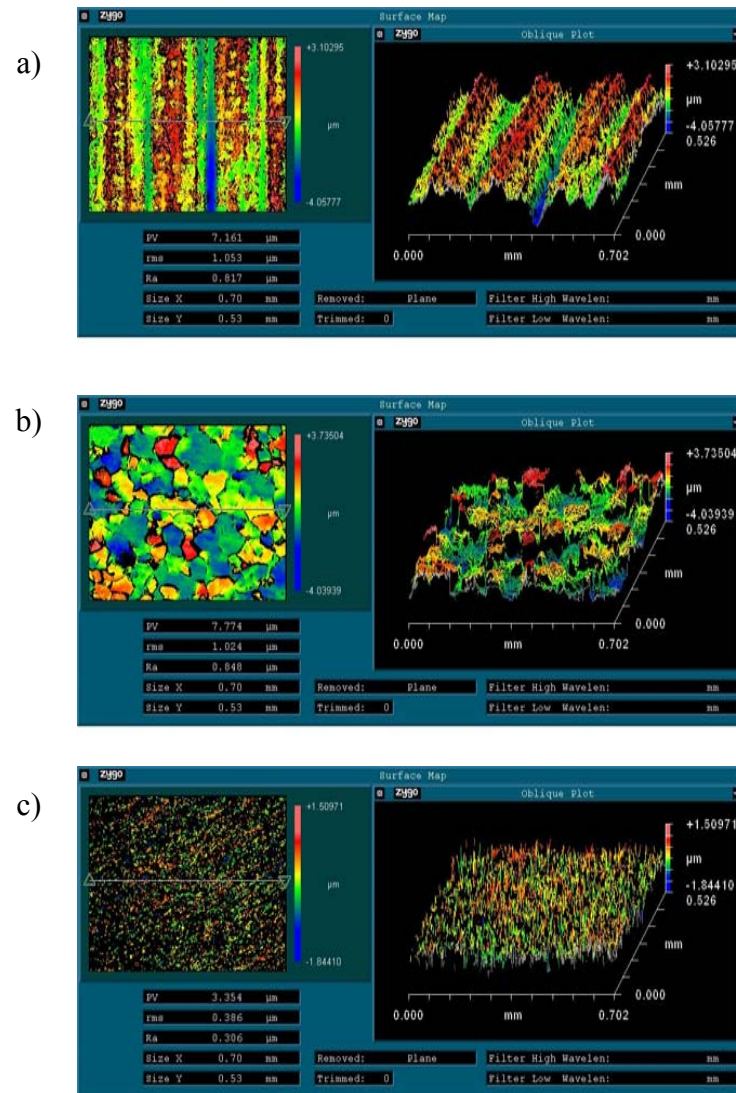


Figure 1: Initial surface textures of a) as rolled, b) BCP treated and, c) mechanically abraded niobium wafers measured by the Zygo optical profiler. The peak-to-valley (PV) roughnesses of these surfaces are 7.16, 7.74 and 3.35 μm , respectively.

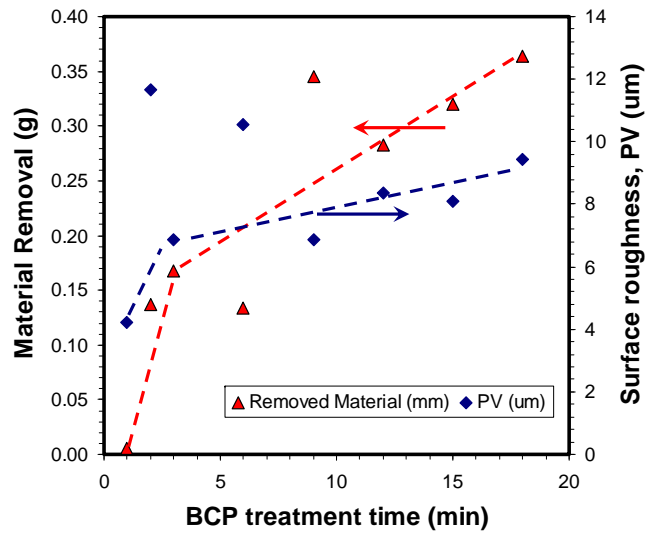


Figure 2: Amount of material removed, and PV roughness of the surface for different durations of BCP treatments.

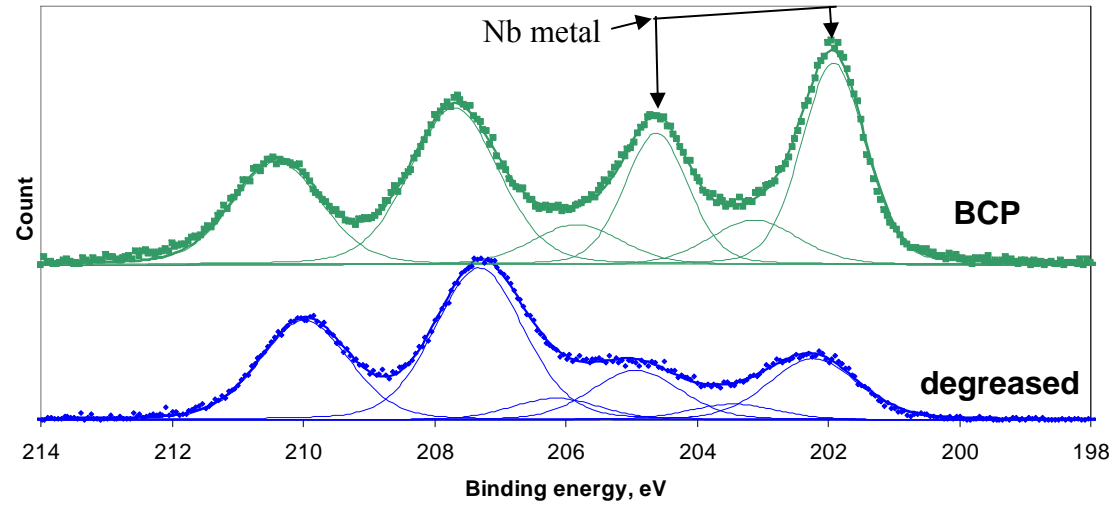


Figure 3: FWHM of the metal peaks decreases to 1.15 eV from 1.60 eV indicating that Nb surface is more ordered after BCP treatment.

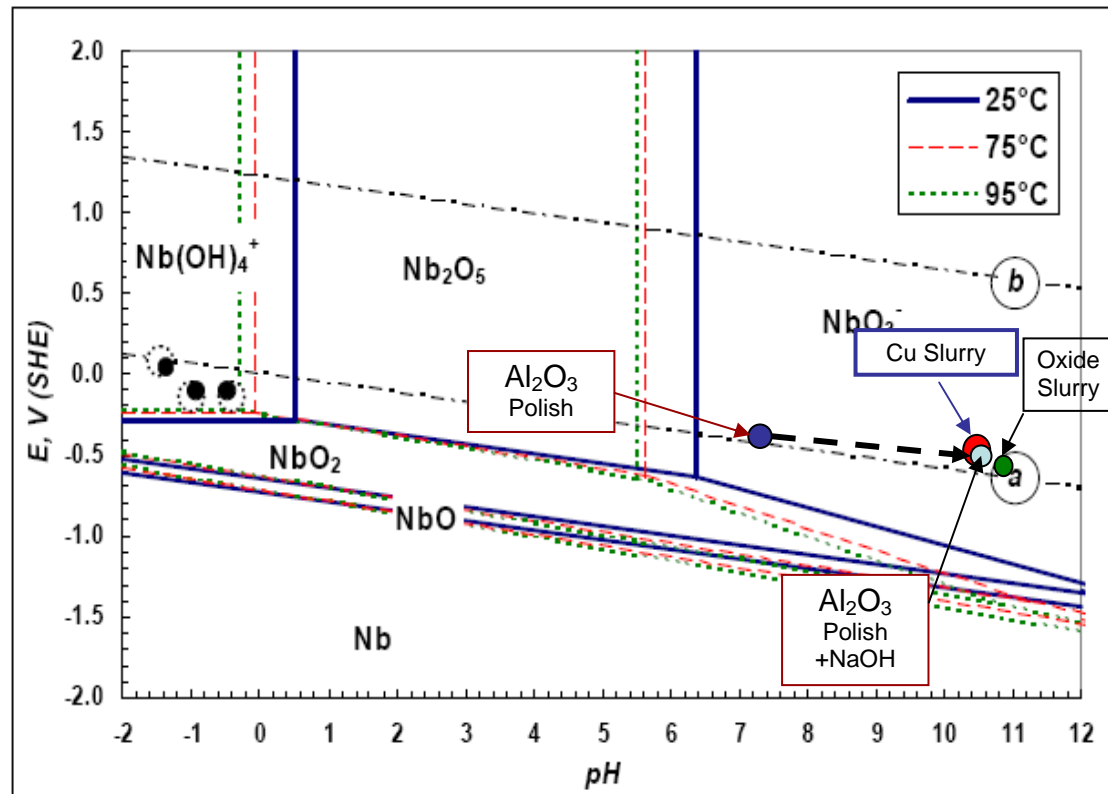
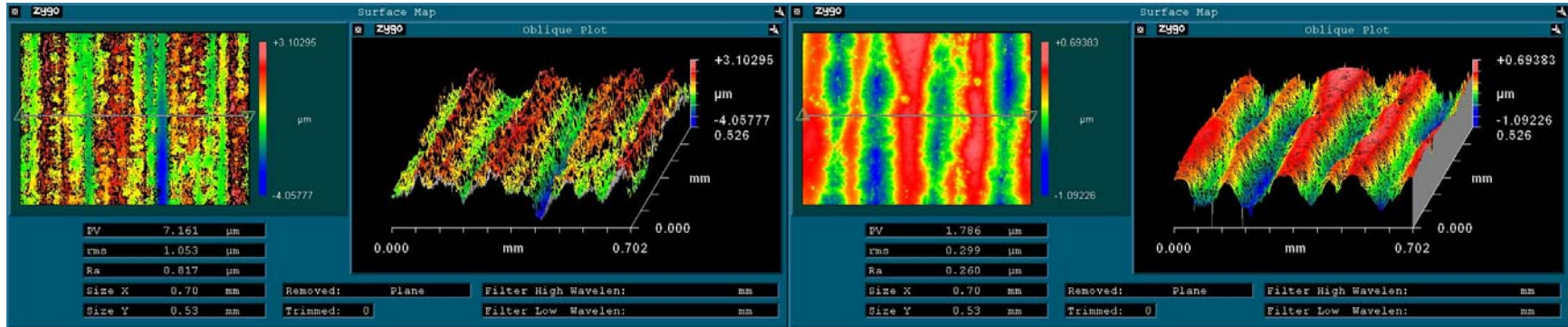
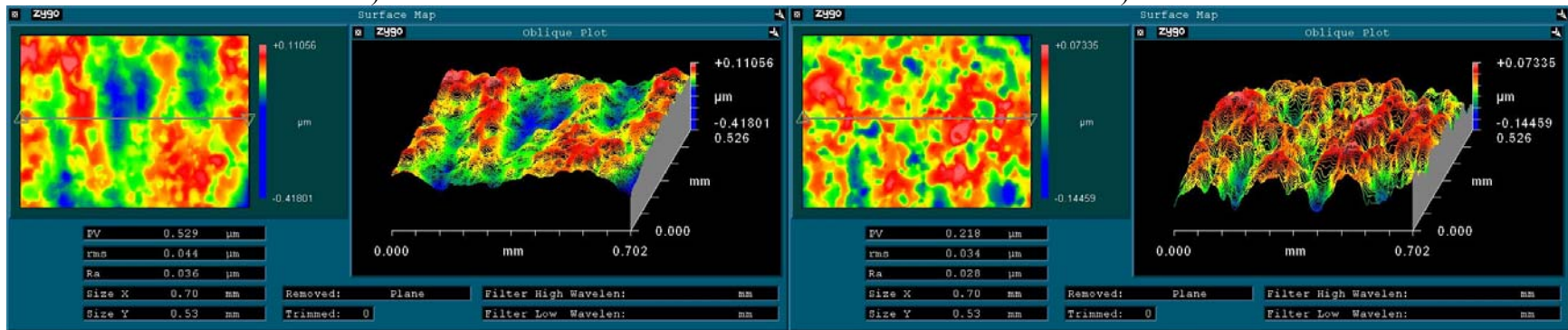


Figure 4: Pourbaix diagram for Nb-H₂O system at 25, 75, and 95°C (Asselin et al. (20)). Lines a and b represent hydrogen evolution and oxygen reduction, respectively. Note that the pH and the OCP of the slurries used in this work are marked on this diagram. pH of alumina polish was adjusted to 10 in order to position this polish in the operational region of oxide slurry. Figure is modified from Asselin et al. (20) with permission from Elsevier.



a) 0 min

b) 42 min



c) 60 min

d) 71 min

Figure 5: Progression of surface roughness in test-1 at time intervals of a) 0, b) 42, c) 60, and d) 71 minutes. This surface was not treated initially, and the outcome of the initial roller marks can be seen in a).

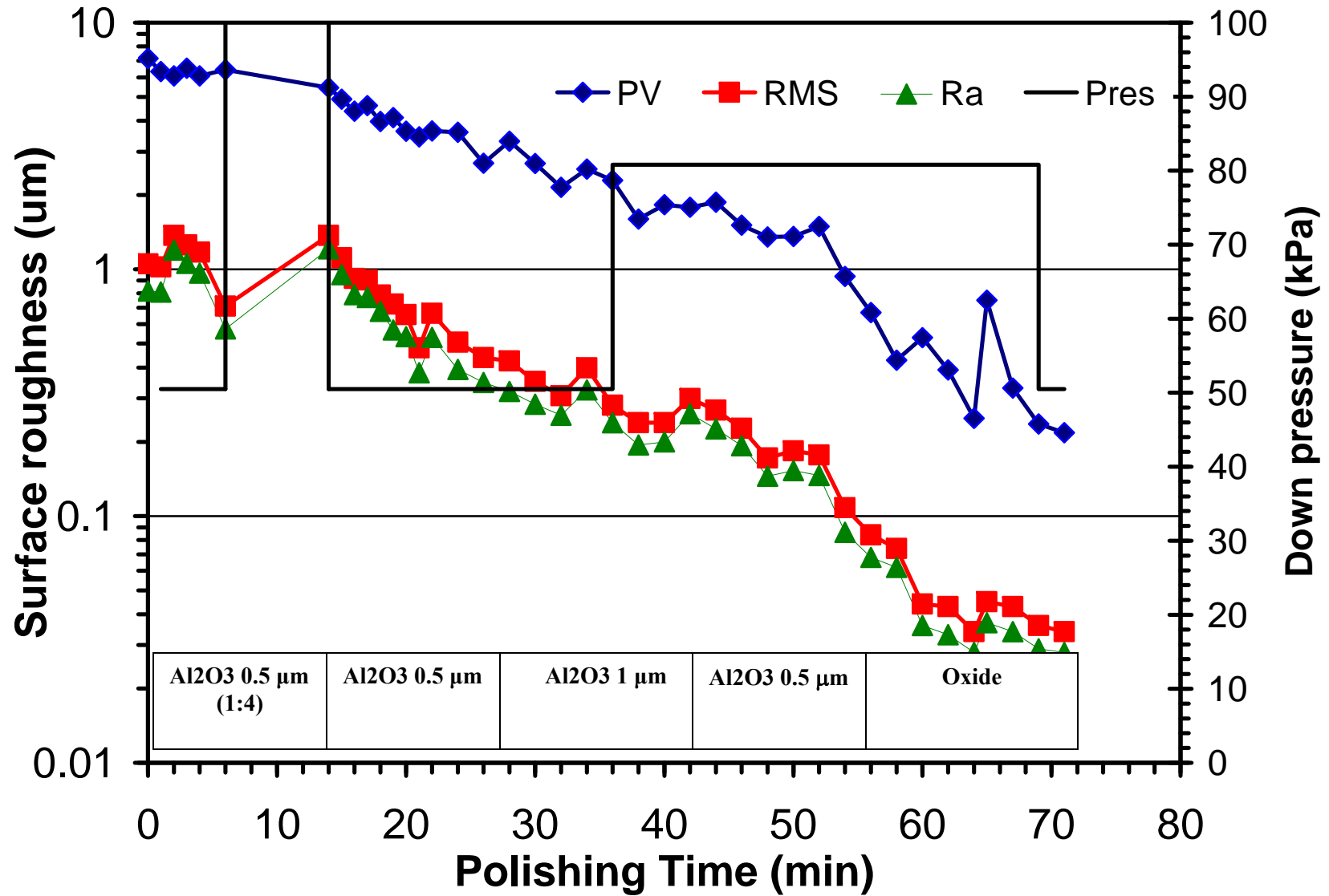
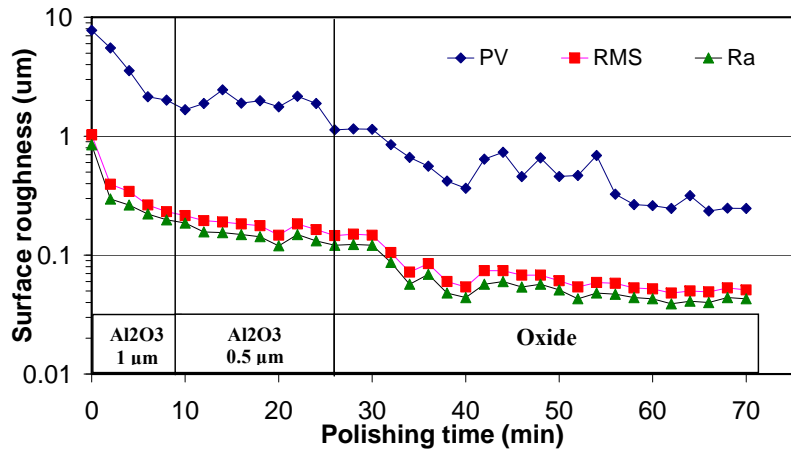
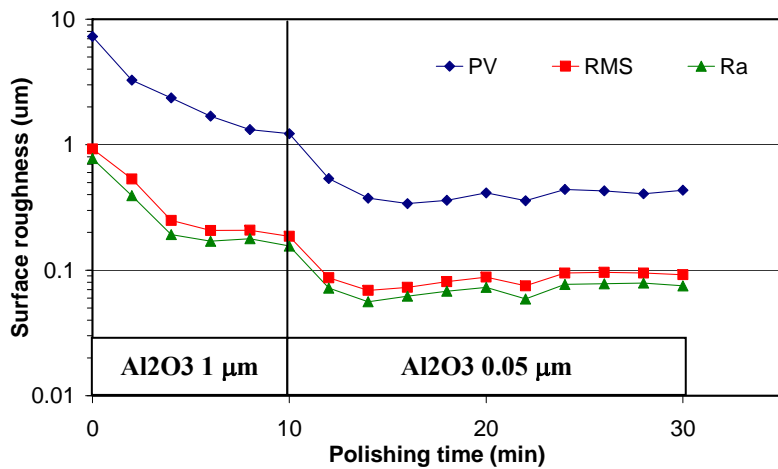


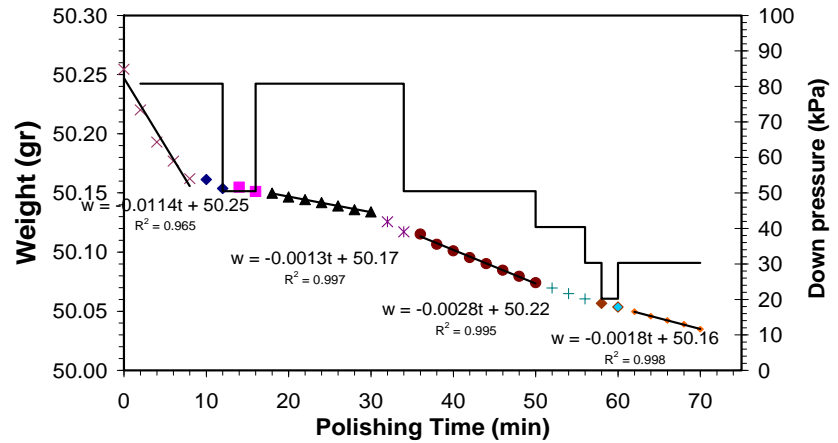
Figure 6: Change in surface roughness due to polishing, over time for a Nb-wafer with as rolled surface.



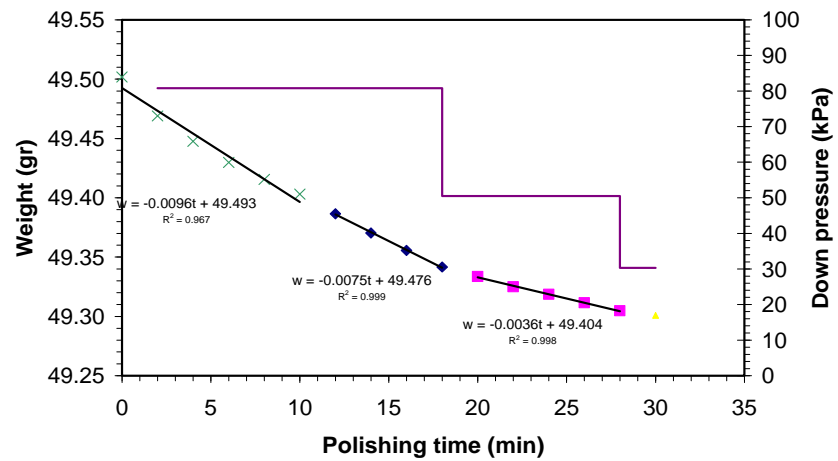
a) Test-2: Oxide-slurry finish



c) Test-3: 50 nm Alumina finish

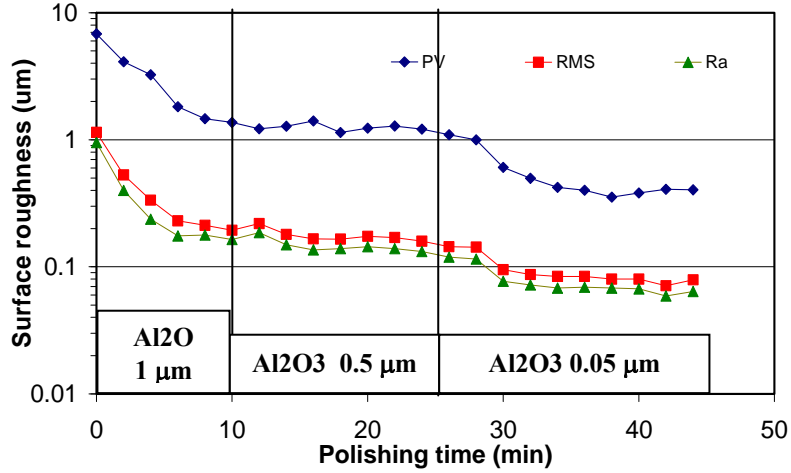


b) Test-2: Oxide-slurry finish

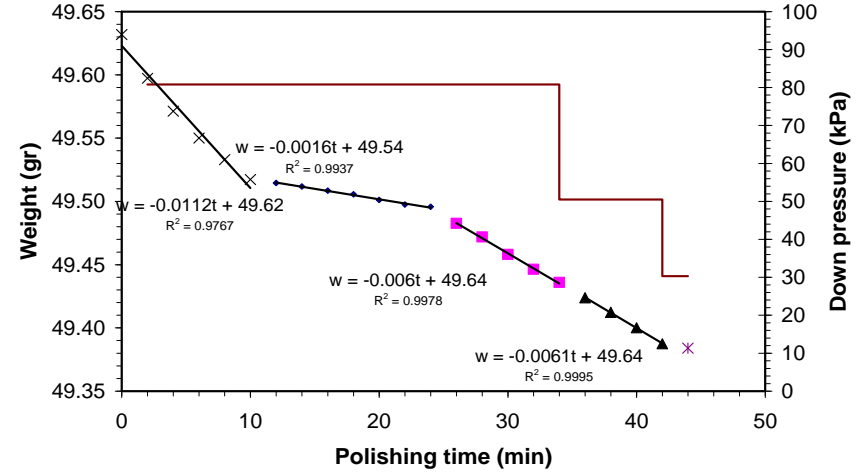


d) Test-3: 50 nm Alumina finish

Figure 7

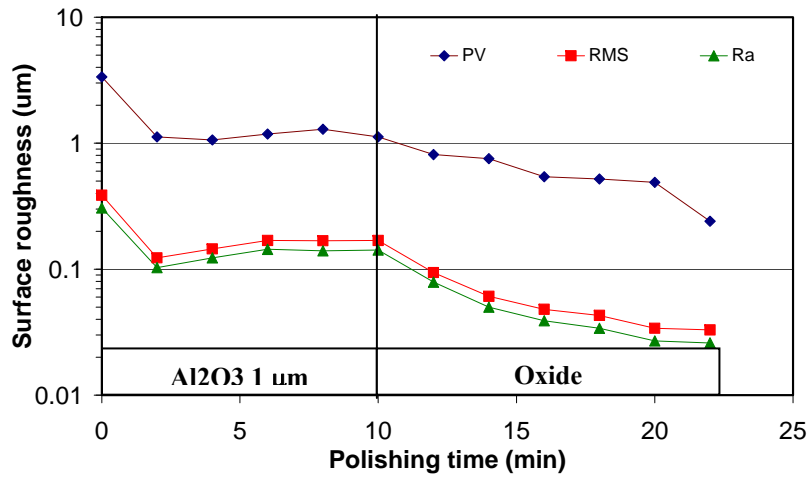


e) Test-4: 50 nm Alumina finish

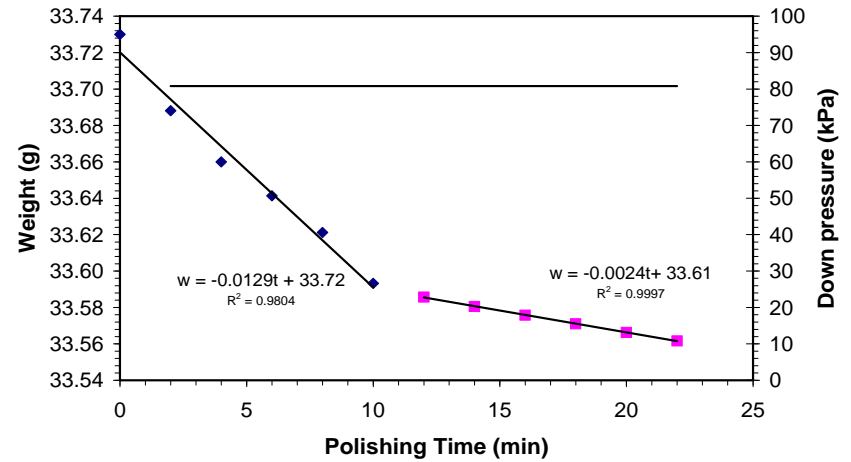


f) Test-4: 50 nm Alumina finish

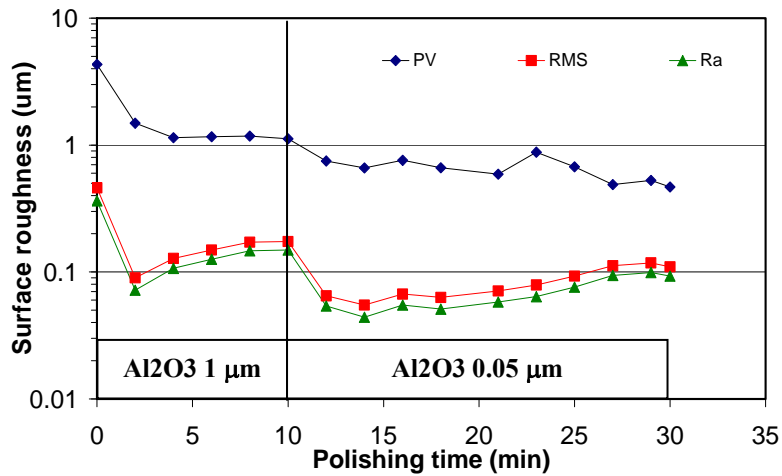
Figure 7: (ctd.) Change in surface roughness due to polishing, over time for Nb-wafers which were initially prepared by a BCP treatment in tests 2-4.



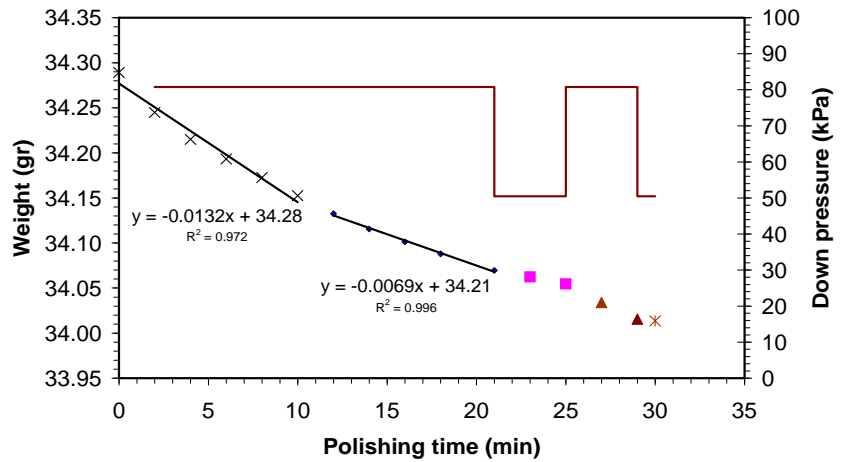
a) Test-5: Oxide-slurry finish



b) Test-5: Oxide-slurry finish

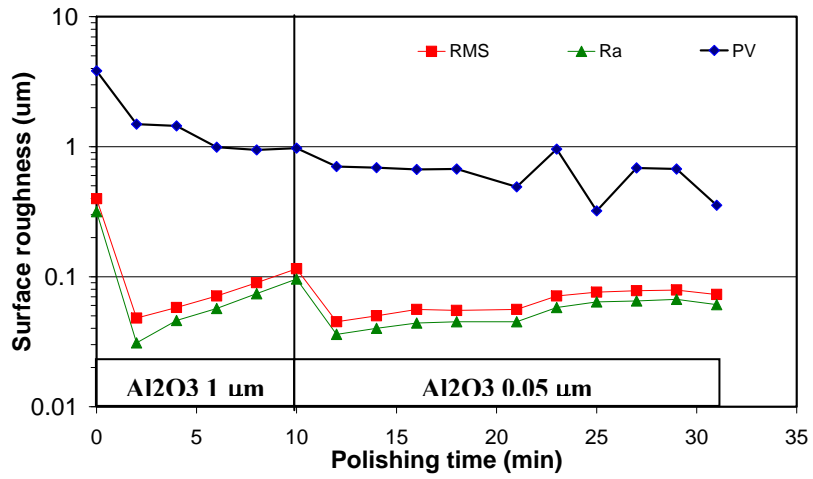


c) Test-6: 50 nm Alumina finish

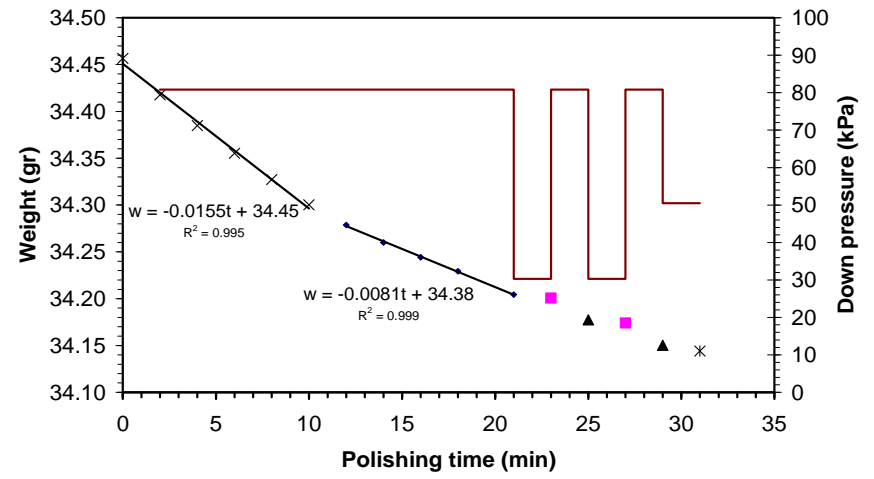


d) Test-6: 50 nm Alumina finish

Figure 8



e) Test-7: 50 nm Alumina finish



f) Test-7: 50 nm Alumina finish

Figure 8: (ctd) Change in surface roughness due to polishing, over time for Nb-wafers which were initially prepared by a mechanical abrasion treatment in tests 5-7.

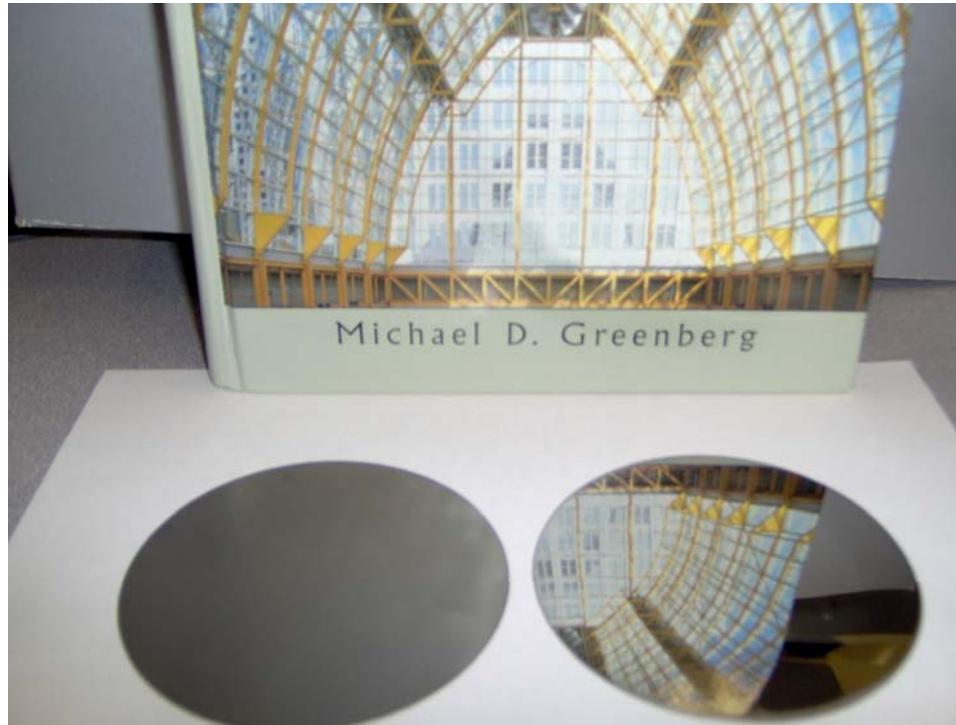
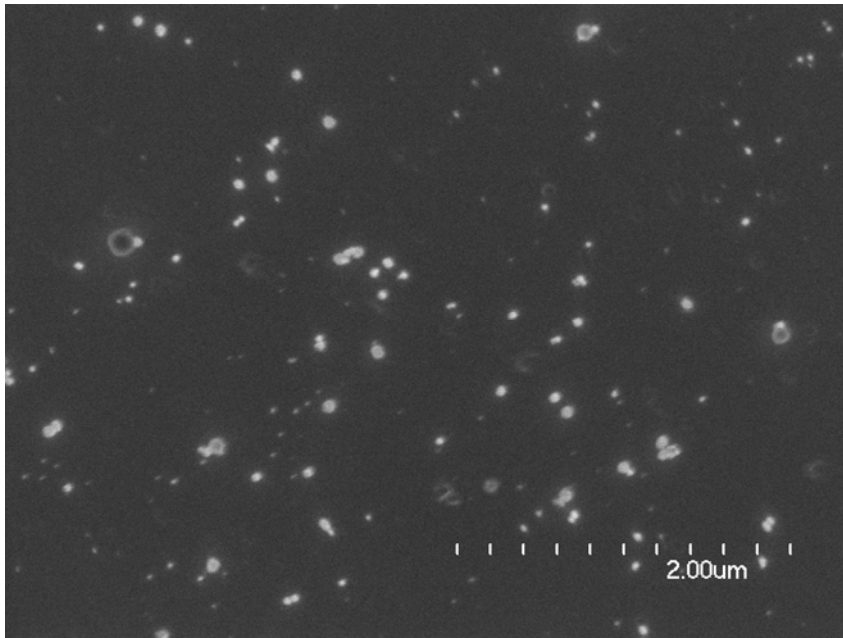
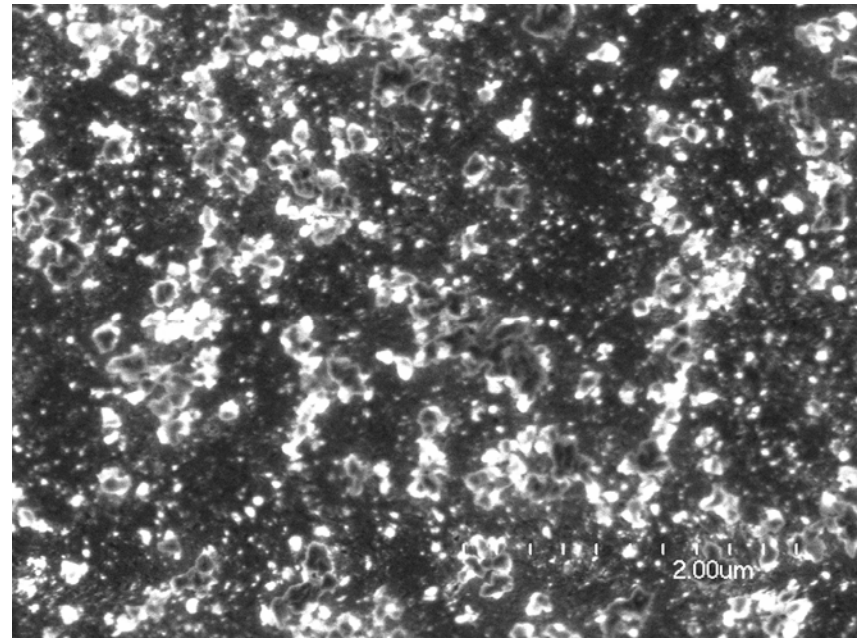


Figure 9: Light reflection from an unpolished Niobium wafer is compared to a polished niobium wafer, finished with an oxide-slurry. The polished wafer on the right is nearly mirror smooth.



a) test-2: Oxide-slurry finish



b) test-3: 50 nm Alumina finish

Figure 10: The SEM images of the final surfaces for tests -2 and -3 at 25K magnification.